[1.] Jimit R. PATEL, [2.] Gunamani DEHERI

A STUDY OF DIFFERENT POROUS STRUCTURES ON THE PERFORMANCE OF A MAGNETIC FLUID BASED ROUGH POROUS TILTED PAD BEARING

[1-2.] Department of Mathematics, Sardar Patel University, Vallabh Vidyanagar, Gujarat, INDIA

ABSTRACT: This article aims to analyze the effect of different porous structures on the behaviour of a porous rough tilted pad bearing in the presence of a magnetic fluid lubricant. The globular sphere model of Kozeny- Carman and the capillary fissures model of Irmay have been adopted to study the porosity effect. A stochastic random variable characterizes the transverse surface roughness of the bearing surfaces. Making use of Christensen and Tonder's stochastic model for roughness the generalized Reynolds equation is derived. The expression for pressure distribution is obtained by resorting to suitable boundary conditions. Then the load carrying capacity of the bearing system is calculated. The results presented in graphical form indicate that the magnetization enhances the performance of the bearing system. Although, the effect of transverse roughness is found to be adverse in general there exist some scopes to obtain relatively better performance at least in the case of negatively skewed roughness. Kozeny-Carman model for porosity scores over Irmay's model from performance point of view.
Keywords: tilted pad bearing, roughness, magnetic fluid, porous structures

1. INTRODUCTION

Capitao [6] carried out a full scale experimental programme to investigate the influence of fluid film turbulence on the performance of the tilting pad self-equalization type thrust bearing. Glavatskih [12] reported the results of the experimental investigation into the steady state performance characteristics of a tilting pad thrust bearing typical of design for general use. The effect of operating conditions on bearing performance was discussed. A small radial temperature variation was observed in the collar. It was also found that the pressure profiles changed with the temperature of the supplied oil. Wasilczuk [26] compared the optimum profile hydrodynamic thrust bearing with a typical tilting pad thrust bearing. The experimental results showed a substantial increase in the minimum oil film thickness and lower temperature in the bearing with the elastic thrust pad. This was due to the optimum oil gap profile in the bearing. Heinrichson et al. [13] described the effects of high pressure injection pockets on the operating conditions of tilting pad thrust bearing. This paper experimentally investigated the influence of an oil injection pocket on the pressure distribution and oil film thickness and validated a numerical model with respect to its ability to predict the influence of such a pocket on the pressure distribution and oil film thickness. Yongbin [27] considered a tilted pad thrust slider bearing improved by the boundary slippage. It was found that the most increase in the load carrying capacity by the boundary slippage was around 30% while the most reduction of friction coefficient of the bearing by the boundary slippage was more than 40%.

Sinha and Adamu [25] dealt with the thermal and roughness effect on the performance characteristics of an infinite tilted pad slider bearing. It was observed that the load carrying capacity due to roughness effect for both the models was more than due to combined effect for a non-parallel slider bearing. It was also established that the load carrying capacity due to the

combined effect was less than the load due to thermal effect for the longitudinal roughness and it was opposite for transverse roughness. Adamu and Sinha [1] modified the above analysis and analyzed the thermal and roughness effect on different performance characteristics of an infinitely long tilted pad slider considering heat conduction through both the pad and slider. Here the irregular domain of the fluid due to roughness was mapped on to a regular domain, so that numerical method was easily adopted. The Reynolds equation for pressure distribution and the heat conduction equation on the pad slider were solved using finite difference method to obtain the bearing characteristics.

Chiang et al. [7] studied the performance of a magneto hydrodynamic tilted bearing with surface roughness lubricated by a ferrofluid. According to the results compared with the Newtonian fluids the tilted bearing lubricated with magnetic ferrofluid had the higher built up pressure distribution and load carrying capacity. The responding time decreased with increasing mean values associated with the roughness. Shukla and Deheri [24] proposed to study the magnetic fluid lubrication of a rough tilted pad slider bearing. It was concluded that the adverse effect of transverse roughness could be minimized to some extent by the positive effect of magnetization which remained enhanced in the case of negatively skewed roughness. Patel and Deheri [20] discussed the comparison of various porous structures on the performance of a magnetic fluid based transversely rough short bearing. Patel and Deheri [21] dealt with the analytical solution for pressure, load and friction for a magnetic fluid based double layered porous slider bearing. It was found that the magnetization tried to compensate the adverse effect of roughness for a large range of combined porous structures. Patel and Deheri [22] presented an analytical solution for the performance characteristics of a magnetic fluid based double layered porous rough slider bearing. It was noticed that the increased load carrying capacity owing to double layered gets enhanced due to the magnetic fluid lubricant and this goes a long way in reducing the adverse effect of roughness in the case of Kozeny-Carman model.

Here it has been sought to analyse the effect of various porous structures on the magnetic fluid lubrication of a rough porous tilted pad bearing.

2. ANALYSIS

Figure 1 shows the geometry of the Tilted Pad bearing. The gap h increases with x, hence the runner has to move towards the origin with its velocity –U. Here the minimum film thickness is h_0 and maximum h_1. The position of h_0 is distance H from the origin and h_1 is $H + B$ away. By similarity of triangles one obtains,
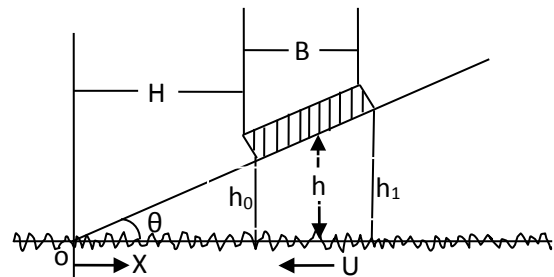
Figure 1: Configuration of the bearing system

$$h = \frac{x h_0}{H}, H = B\left(\frac{h_0}{h_1 - h_0}\right) = \frac{B}{K}, K = \frac{h_1 - h_0}{h_0}$$

The lubricant film is considered to be isoviscous and incompressible and the flow is laminar. It is assumed that the bearing surfaces are transversely rough. According to the stochastic model of Christensen and Tonder [8, 9, 10], the thickness $h(x)$ of the lubricant film is considered as

$$h(x) = \bar{h}(x) + h_s$$

where $\bar{h}(x)$ is the mean film thickness and h_s is the deviation from the mean film thickness characterizing the random roughness of the bearing surfaces. h_s is governed by the probability density function

$$f(h_s) = \begin{cases} \frac{35}{32 c_1}\left(1 - \frac{h_s^2}{c_1^2}\right)^3 & , -c_1 \le h_s \le c_1 \\ 0 & , \text{ elsewhere} \end{cases}$$

wherein c_1 is the maximum deviation from the mean film thickness. The mean α, the standard deviation σ and the parameter ε which is the measure of symmetry of the random variable h_s, are defined and discussed in Christensen and Tonder [8, 9, 10].

Agrawal [2] considered the magnetic fluid lubrication effect by taking the magnetic field oblique to the stator. The effect of various forms of magnitude of the magnetic field has been discussed by

Prajapati [23]. Following this discussion therein, the magnitude of the magnetic field is considered to be

$$M^2 = kB\left(\frac{h}{h_0} - 1\right)\left(K + 1 - \frac{h}{h_0}\right)$$

where k is a suitably chosen constant from dimensionless point of view so as to produce a magnetic field of strength over 10^{-23}(Bhat and Deheri [3]).

Under the usual assumptions of hydro magnetic lubrication (Bhat [4], Prajapati [23], Deheri et al. [11]) the Reynolds equation governing the pressure distribution is obtained as

$$\frac{d}{dx}\left(p - \frac{\mu_0\,\bar\mu M^2}{2}\right) = -6U\eta\frac{h - \bar h}{g(h)} \tag{1}$$

where $g(h) = h^3 + 3h^2\alpha + 3(\sigma^2 + \alpha^2)h + 3\sigma^2\alpha + \alpha^3 + \varepsilon + 12\psi l_1$.

while μ_0 is the magnetic susceptibility, $\bar\mu$ is the free space permeability, μ is the lubricant viscosity and ψ is permeability of porous region, $\bar h$ is a constant to be determined and l_1 is layer thickness.

The associated boundary conditions are

$$p = 0 \text{ at } h = h_0 \text{ and } h = h_1 \tag{2}$$

Case 1: (A globular sphere model)

A porous material is filled with globular spherical particles (a mean particle size D_c) as shown in Figure A.

The Kozeny-Carman equation is well known in the fluid dynamics. This model when applied to laminar flow, yields better results for pressure drop. The pressure gradient is treated to be linear. Liu [15], Patel and Deheri [17] suggest that the use of Kozeny-Carman formula turns in the relation
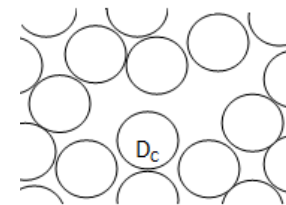
Figure A: Structure model of porous sheets given by Kozeny-Carman

$$\psi = \frac{D_c^2 e^3}{72(1 - e)^2}\frac{l}{l'}$$

where e is the porosity and $\frac{l'}{l}$ is the length ratio. From experimental investigations the length ratio veers around 2.5 under suitable situations. Thus, the Kozeny-Carman formula takes the form (Patel and Deheri [19])

$$\psi = \frac{D_c^2 e^3}{180(1 - e)^2}$$

Introducing the dimensionless quantities

$$l^* = \frac{l}{l'}, P = \frac{h_0^2}{6U\eta B}p, h^* = \frac{h}{h_0}, \mu^* = \frac{k\mu_0\bar\mu h_0^2}{U\eta}, \lambda = \frac{\bar h}{h_0}, \bar\sigma = \frac{\sigma}{h_0}, \bar\alpha = \frac{\alpha}{h_0}, \bar\varepsilon = \frac{\varepsilon}{h_0^3}, \bar\psi = \frac{D_c^2 l_1}{h_0^3},$$

$$a = 3\bar\alpha, b = 3(\bar\alpha^2 + \bar\sigma^2), c = \bar\alpha^3 + 3\bar\sigma^2\bar\alpha + \bar\varepsilon + \frac{\bar\psi\, l^* e^3}{6(1 - e)^2}, J = \sqrt[3]{-2a^3 + 3\sqrt{3}K_1 + 9ab - 27c},$$

$$K_1 = \sqrt{4a^3c - a^2b^2 - 18abc + 4b^3 + 27c^2}, J_1 = \frac{J}{3\sqrt[3]{2}} - \frac{\sqrt[3]{2}(3b - a^2)}{3\,J} - \frac{a}{3}, Q = \frac{J}{6\sqrt[3]{2}}, A = \frac{J_1}{S},$$

$$R = \frac{(3b - a^2)}{32^{2/3}\,J}, J_2 = -2Q + 2R - \frac{2a}{3}, J_3 = 4Q^2 + 4QR + 4R^2 + 2Q\frac{a}{3} - 2R\frac{a}{3} + \frac{a^2}{9}, B = -A,$$

$$S = J_1^2 - J_1J_2 + J_3, C = \frac{J_3}{S}, A_1 = \frac{1}{S}, B_1 = -A_1, C_1 = \frac{J_2 - J_1}{S}, D = \ln\left(\frac{1 - J_1}{K + 1 - J_1}\right),$$

$$E = \ln\left(\frac{1 - J_2 + J_3}{(K + 1)^2 - J_2(K + 1) + J_3}\right), F = \tan^{-1}\left(\frac{-2K\sqrt{4J_3 - J_2^2}}{(4J_3 - J_2^2) + (2 - J_2)(2(K + 1) - J_2)}\right),$$

$$G = \frac{J_2B + 2C}{\sqrt{4J_3 - J_2^2}}, q = \frac{J_2B_1 + 2C_1}{\sqrt{4J_3 - J_2^2}}, \lambda = \frac{(AD + (B/2)E + GF)}{(A_1D + (B_1/2)E + qF)}, P_1 = \ln\left(\frac{h^* - J_1}{1 - J_1}\right),$$

$$P_2 = \ln\left(\frac{h^{*2} - J_2h^* + J_3}{1 - J_2 + J_3}\right), P_3 = \tan^{-1}\left(\frac{2(h^* - 1)\sqrt{4J_3 - J_2^2}}{(4J_3 - J_2^2) + (2 - J_2)(2h^* - J_2)}\right)$$

$$w_1 = (K + 1 - J_1)(-D) - K, I = \tan^{-1}\left(\frac{2(K+1) - J_2}{\sqrt{4J_3 - J_2^2}}\right) - \tan^{-1}\left(\frac{2 - J_2}{\sqrt{4J_3 - J_2^2}}\right),$$

$$N = \ln\left(1 + \left(\frac{2 - J_2}{\sqrt{4J_3 - J_2^2}}\right)^2\right) - \ln\left(1 + \left(\frac{2(K+1) - J_2}{\sqrt{4J_3 - J_2^2}}\right)^2\right),$$

$$w_2 = \sqrt{4J_3 - J_2^2}\, I + \left(\frac{2(K+1) - J_2}{2}\right)(-E) - 2K, w_3 = \left(\frac{2(K+1) - J_2}{2}\right)I + \frac{\sqrt{4J_3 - J_2^2}}{4}\, N. \quad (3)$$

and the non-dimensional form of roughness term

$$g(\overline{h}) = h^{*3} + 3h^{*2}\overline{\alpha} + 3\,(\overline{\sigma}^2 + \overline{\alpha}^2)h^* + 3\overline{\sigma}^2\overline{\alpha} + \overline{\alpha}^3 + \overline{\epsilon} + \frac{\overline{\psi}\, l^* e^3}{6(1 - e)^2},$$

resorting to the boundary conditions (2), the non-dimensional form of the pressure distribution in the case of Kozeny- Carman, is derived as

$$P = \frac{\mu^*}{12}(h^* - 1)(K + 1 - h^*) - \frac{1}{K}\left[(A - \lambda A_1)P_1 + \frac{1}{2}(B - \lambda B_1)P_2 + (G - \lambda q)P_3\right] \quad (4)$$

The load carrying capacity of the bearing system then is determined by

$$W = \frac{h_0^2}{6U\eta LB^2}\, w = \frac{1}{K}\int_{h_0}^{h_1} p\, dh \quad (5)$$

Consequently, the expression for the dimensionless load carrying capacity turns out to be

$$W = \frac{\mu^*}{72}K^2 - \frac{1}{K^2}\left[(A - \lambda A_1)w_1 + \frac{1}{2}(B - \lambda B_1)w_2 + (G - \lambda q)w_3\right] \quad (6)$$

Case-2 :(A capillary fissures model)

Figure B, the model of porous sheets given by Irmay, consists of three sets of mutually orthogonal fissures (a mean solid size D_s). Assuming no loss of hydraulic gradient at the junctions, Irmay [14] obtained the permeability,

$$\psi = \frac{D_s^2\left(1 - (1 - e)^{\frac{2}{3}}\right)}{12(1 - e)}$$

where e is the porosity (Patel and Deheri [18]).
The following non dimensional quantities are introduced in the sequel:
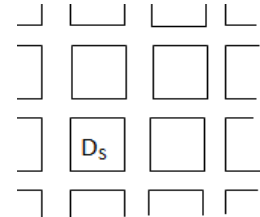
Figure B: Structure model of porous sheets given by Irmay

$$\psi^* = \frac{D_s^2 l_1}{h_0^3}. c^* = \overline{\alpha}^3 + 3\overline{\sigma}^2\overline{\alpha} + \overline{\epsilon} + \frac{\psi^*\left(1 - (1 - e)^{\frac{2}{3}}\right)}{(1 - e)}, J^* = \sqrt[3]{-2a^3 + 3\sqrt{3}K_1^* + 9ab - 27c^*},$$

$$K_1^* = \sqrt{4a^3 c^* - a^2 b^2 - 18abc^* + 4b^3 + 27c^{*2}}, J_1^* = \frac{J^*}{3\sqrt[3]{2}} - \frac{\sqrt[3]{2}(3b - a^2)}{3J^*} - \frac{a}{3}, Q^* = \frac{J^*}{6\sqrt[3]{2}},$$

$$R^* = \frac{(3b - a^2)}{32^{2/3}\, J^*}, J_2^* = -2Q^* + 2R^* - \frac{2a}{3}, J_3^* = 4Q^{*2} + 4Q^*R^* + 4R^{*2} + 2Q^*\frac{a}{3} - 2R^*\frac{a}{3} + \frac{a^2}{9},$$

$$S^* = J_1^{*2} - J_1^*J_2^* + J_3^*, A^* = \frac{J_1^*}{S^*}, B^* = -A^*, C^* = \frac{J_3^*}{S^*}, A_1^* = \frac{1}{S^*}, B_1^* = -A_1^*, C_1^* = \frac{J_2^* - J_1^*}{S^*},$$

$$D^* = \ln\left(\frac{1 - J_1^*}{K + 1 - J_1^*}\right), E^* = \ln\left(\frac{1 - J_2^* + J_3^*}{(K+1)^2 - J_2^*(K+1) + J_3^*}\right), \lambda = \frac{(A^*D^* + (B^*/2)E^* + G^*F^*)}{(A_1^*D^* + (B_1^*/2)E^* + q^*F^*)},$$

$$F^* = \tan^{-1}\left(\frac{-2K\sqrt{4J_3^* - J_2^{*2}}}{(4J_3^* - J_2^{*2}) + (2 - J_2^*)(2(K+1) - J_2^*)}\right), q = \frac{J_2^*B_1^* + 2C_1^*}{\sqrt{4J_3^* - J_2^{*2}}}, P_1^* = \ln\left(\frac{h^* - J_1^*}{1 - J_1^*}\right),$$

$$P_2^* = \ln\left(\frac{h^{*2} - J_2^*h^* + J_3^*}{1 - J_2^* + J_3^*}\right), P_3^* = \tan^{-1}\left(\frac{2(h^* - 1)\sqrt{4J_3^* - J_2^{*2}}}{(4J_3^* - J_2^{*2}) + (2 - J_2^*)(2h^* - J_2^*)}\right), G^* = \frac{J_2^*B^* + 2C^*}{\sqrt{4J_3^* - J_2^{*2}}},$$

$$w_1^* = (K + 1 - J_1^*)(-D^*) - K, I^* = \tan^{-1}\left(\frac{2(K+1) - J_2^*}{\sqrt{4J_3^* - J_2^{*2}}}\right) - \tan^{-1}\left(\frac{2 - J_2^*}{\sqrt{4J_3^* - J_2^{*2}}}\right),$$

$$N^* = \ln\left(1 + \left(\frac{2 - J_2^*}{\sqrt{4J_3^* - J_2^{*2}}}\right)^2\right) - \ln\left(1 + \left(\frac{2(K + 1) - J_2^*}{\sqrt{4J_3^* - J_2^{*2}}}\right)^2\right),$$

$$w_2^* = \sqrt{4J_3^* - J_2^{*2}}\, I^* + \left(\frac{2(K + 1) - J_2^*}{2}\right)(-E^*) - 2K, w_3^* = \left(\frac{2(K + 1) - J_2^*}{2}\right)I^* + \frac{\sqrt{4J_3^* - J_2^{*2}}}{4}\, N^*$$

In view of boundary conditions (2) and making use of non-dimensional form of roughness term

$$g(\bar{h}^*) = h^{*3} + 3h^{*2}\bar{\alpha} + 3\,(\bar{\sigma}^2 + \bar{\alpha}^2)h^* + 3\bar{\sigma}^2\bar{\alpha} + \bar{\alpha}^3 + \bar{\varepsilon} + \frac{\psi^*\left(1 - (1 - e)^{\frac{2}{3}}\right)}{(1 - e)},$$

the dimensionless pressure distribution for Irmay model is found to be

$$P^* = \frac{\mu^*}{12}(h^* - 1)(K + 1 - h^*) - \frac{1}{K}\left[(A^* - \lambda^* A_1^*)P_1^* + \frac{1}{2}(B^* - \lambda^* B_1^*)P_2^* + (G^* - \lambda^* q^*)P_3^*\right] \quad (7)$$

From Equation (5), the non-dimensional load carrying capacity is calculated as

$$W^* = \frac{\mu^*}{72}K^2 - \frac{1}{K^2}\left[(A^* - \lambda^* A_1^*)w_1^* + \frac{1}{2}(B^* - \lambda^* B_1^*)w_2^* + (G^* - \lambda^* q^*)w_3^*\right] \quad (8)$$

3. RESULTS AND DISCUSSIONS

It can be observed that the pressure increases by $\frac{\mu^*}{12}(h^* - 1)(K + 1 - h^*)$ while the increase in load carrying capacity is $\frac{\mu^*}{72}K^2$ due to the magnetic fluid lubrication as compared to the case of conventional lubricants. Further, it is concluded that at least there is 1.38% increase in the load due to the magnetic fluid. Besides, as the expression determining the dimensionless load carrying capacity is linear with respect to magnetization μ^*, increasing values of μ^* could lead to increased load carrying capacity. In the absence of roughness this investigation reduces to the porosity effect on different performance characteristics of a magnetic fluid based Tilted pad slider bearing. Lastly, taking μ^* to be zero this investigation reduces to the discussion of Cameron [5] and Majumdar [16] in the absence of porosity.
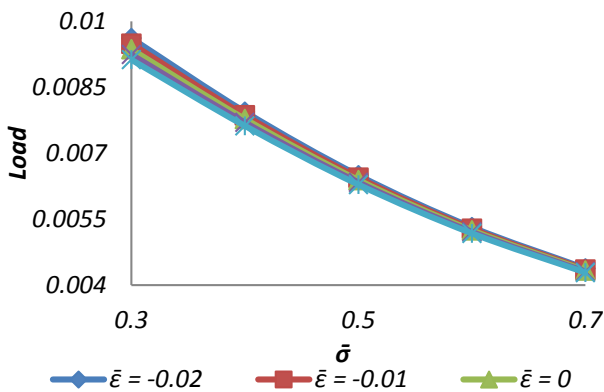
Figure 2: Variation of Load carrying capacity with respect to $\bar{\sigma}$ and $\bar{\varepsilon}$.
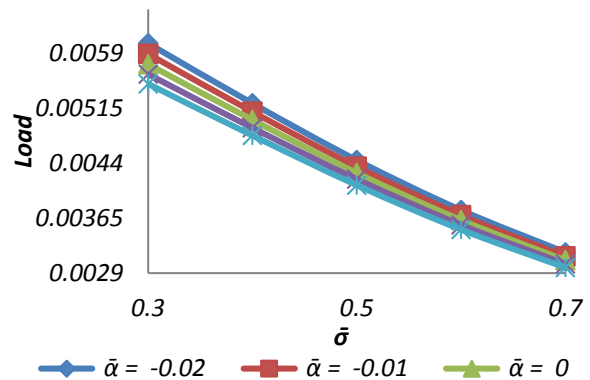
Figure 3: Variation of Load carrying capacity with respect to $\bar{\sigma}$ and $\bar{\alpha}$.
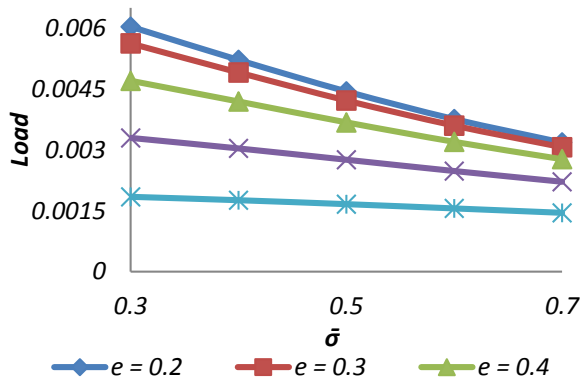
Figure 4: Variation of Load carrying capacity with respect to $\bar{\sigma}$ and e.
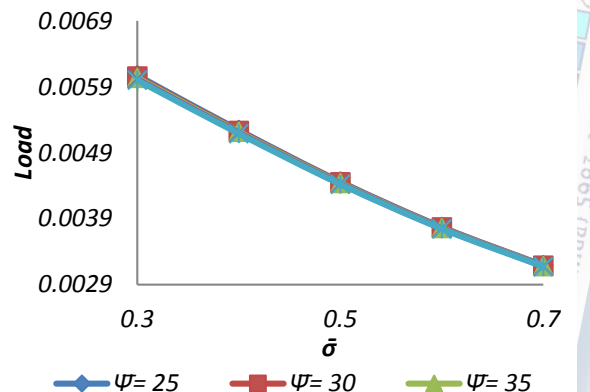
Figure 5: Variation of Load carrying capacity with respect to $\bar{\sigma}$ and $\bar{\psi}$.
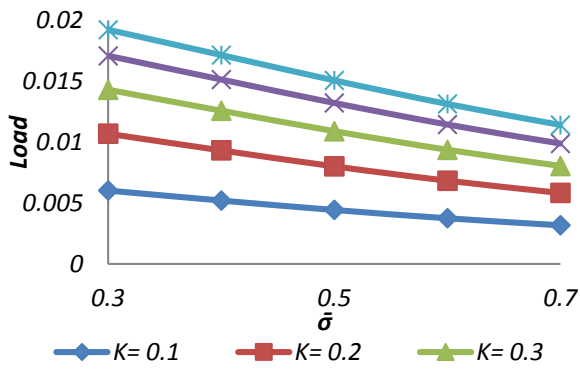
Figure 6: Variation of Load carrying capacity with respect to $\bar{\sigma}$ and K.
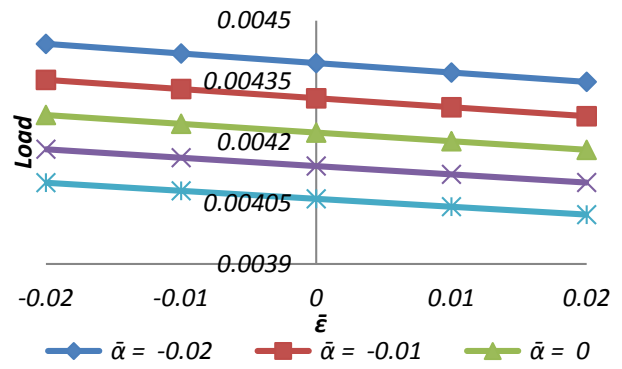
Figure 7: Variation of Load carrying capacity with respect to $\bar{\varepsilon}$ and $\bar{\alpha}$.
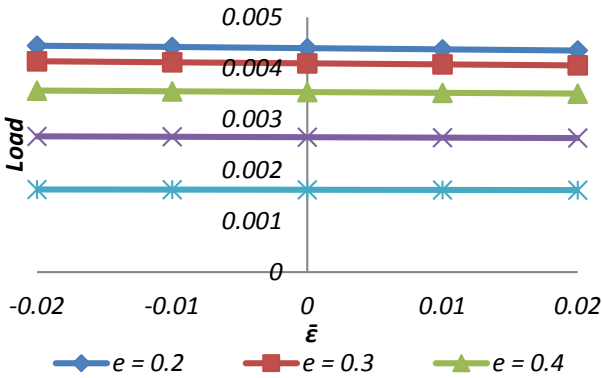
Figure 8: Variation of Load carrying capacity with respect to $\bar{\varepsilon}$ and e.
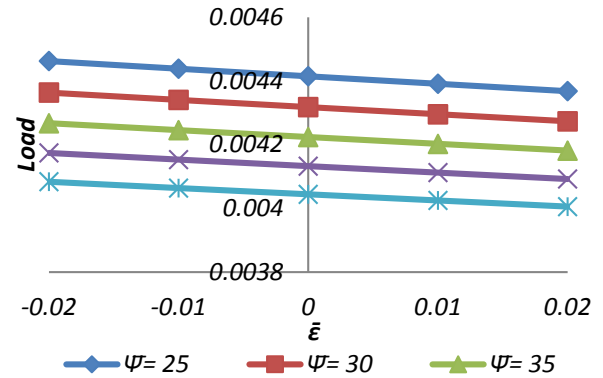
Figure 9: Variation of Load carrying capacity with respect to $\bar{\varepsilon}$ and $\bar{\psi}$.
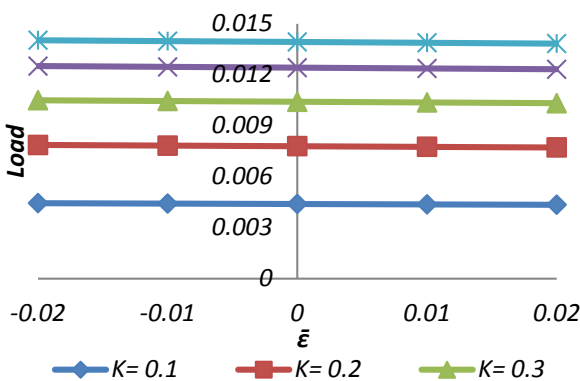
Figure 10: Variation of Load carrying capacity with respect to $\bar{\varepsilon}$ and K.
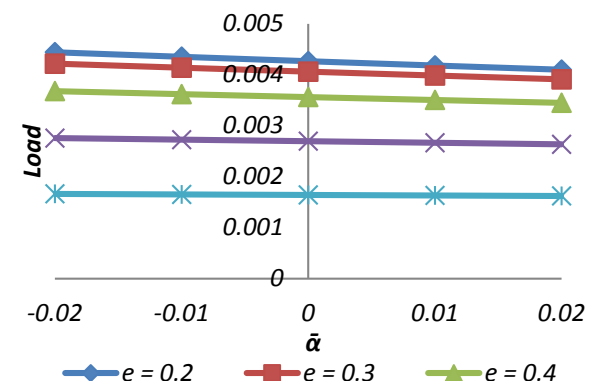
Figure 11: Variation of Load carrying capacity with respect to $\bar{\alpha}$ and e.
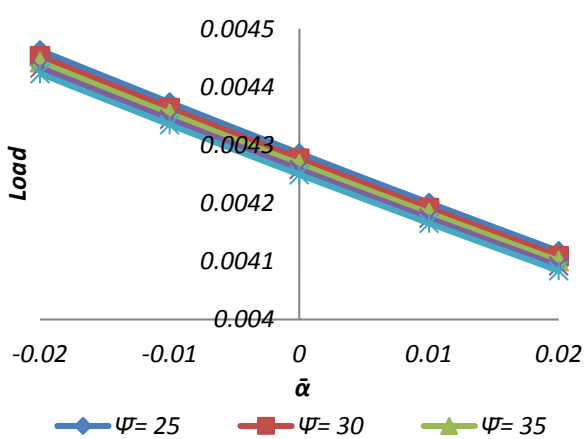
Figure 12: Variation of Load carrying capacity with respect to $\bar{\alpha}$ and $\bar{\psi}$.
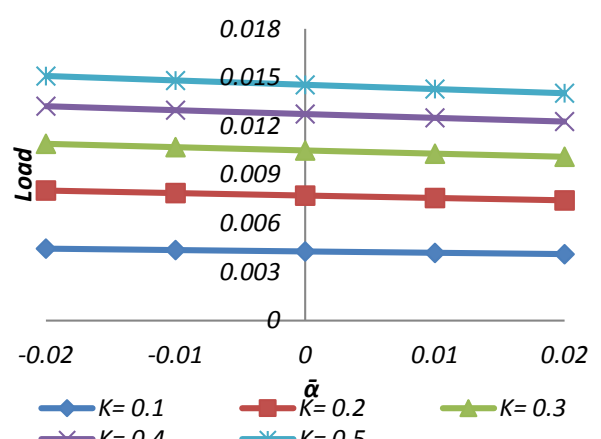
Figure 13: Variation of Load carrying capacity with respect to $\bar{\alpha}$ and K.
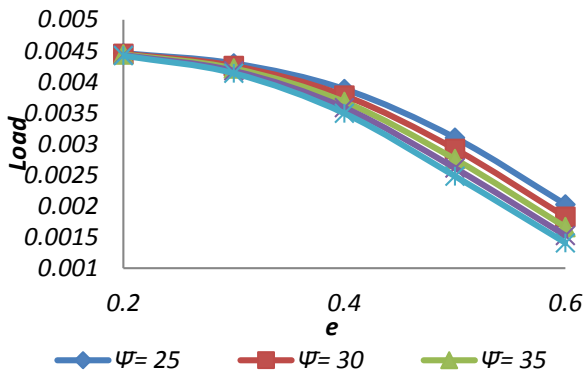
Figure 14: Variation of Load carrying capacity with respect to e and $\bar{\psi}$.
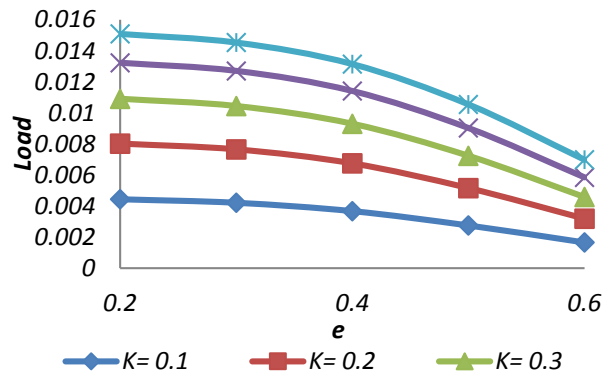
Figure 15: Variation of Load carrying capacity with respect to e and K.
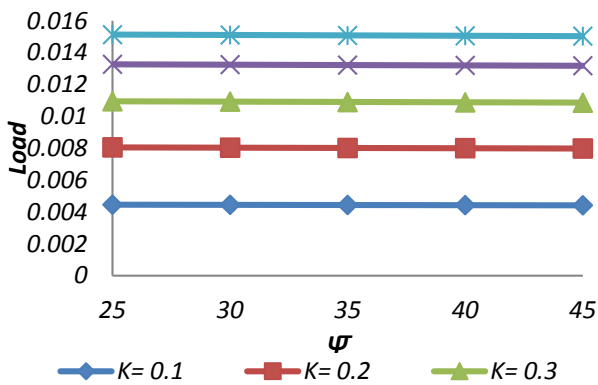
Figure 16: Variation of Load carrying capacity with respect to $\bar{\psi}$ and K.
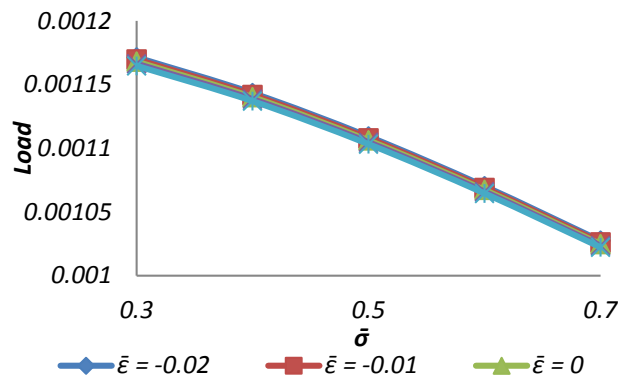
Figure 17: Variation of Load carrying capacity with respect to $\bar{\sigma}$ and $\bar{\varepsilon}$.
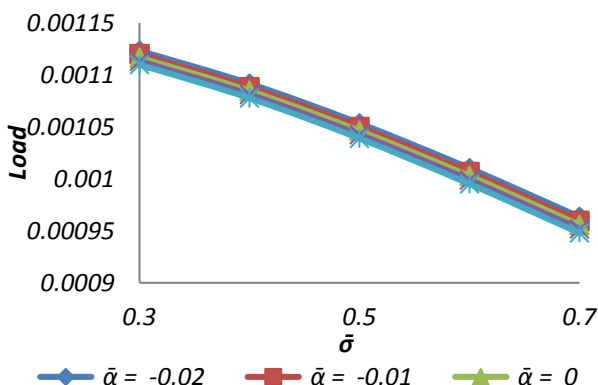
Figure 18: Variation of Load carrying capacity with respect to $\bar{\sigma}$ and $\bar{\alpha}$.
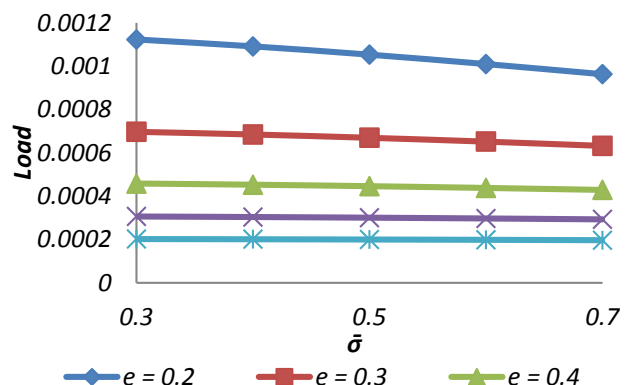
Figure 19: Variation of Load carrying capacity with respect to $\bar{\sigma}$ and e.
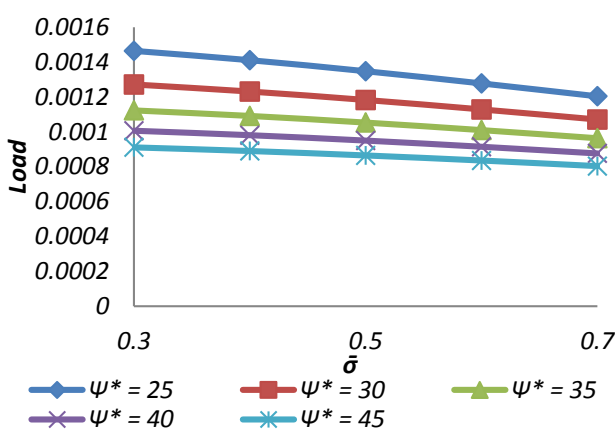
Figure 20: Variation of Load carrying capacity with respect to $\bar{\sigma}$ and ψ^*.
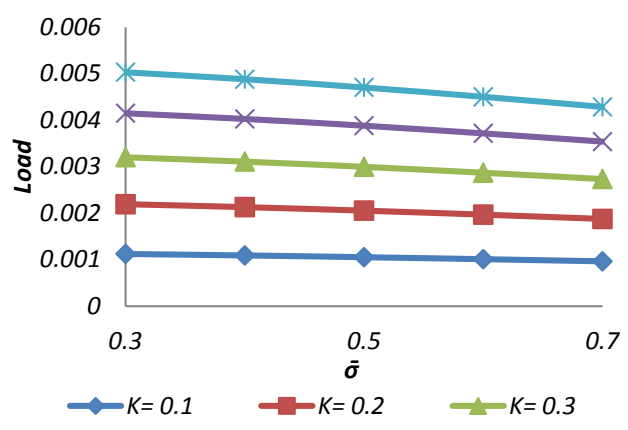
Figure 21: Variation of Load carrying capacity with respect to $\bar{\sigma}$ and K.
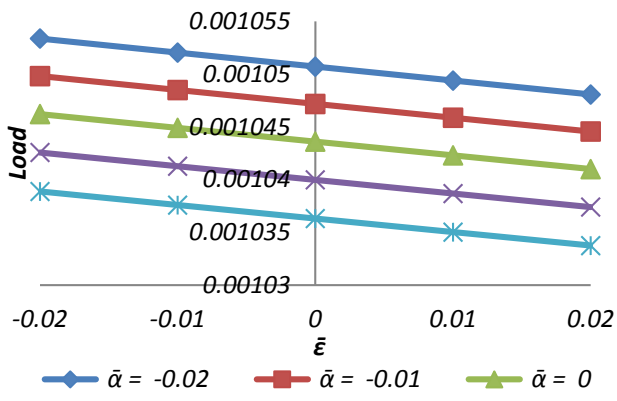
Figure 22: Variation of Load carrying capacity with respect to $\bar{\varepsilon}$ and $\bar{\alpha}$.
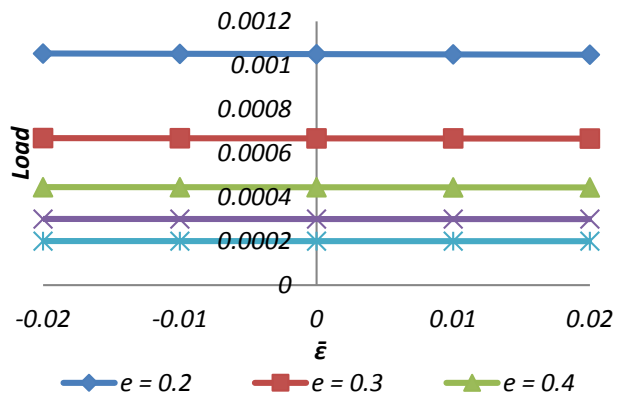
Figure 23: Variation of Load carrying capacity with respect to $\bar{\varepsilon}$ and e.
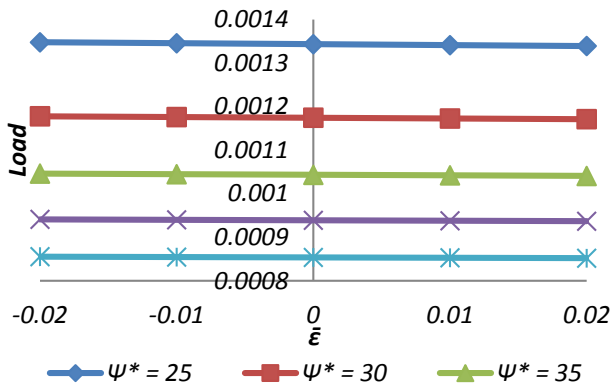
Figure 24: Variation of Load carrying capacity with respect to $\bar{\varepsilon}$ and ψ^*.
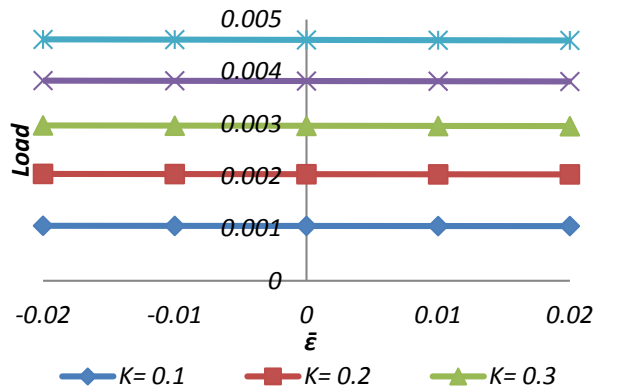
Figure 25: Variation of Load carrying capacity with respect to $\bar{\varepsilon}$ and K.
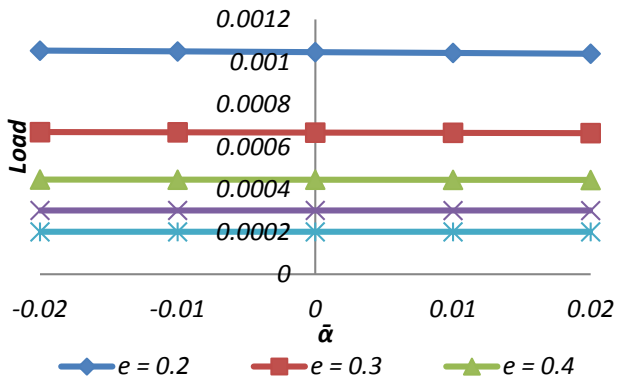
Figure 26: Variation of Load carrying capacity with respect to $\bar{\alpha}$ and e.
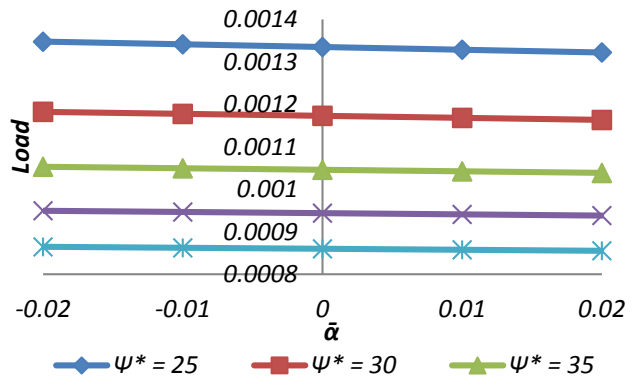
Figure 27: Variation of Load carrying capacity with respect to $\bar{\alpha}$ and ψ^*.
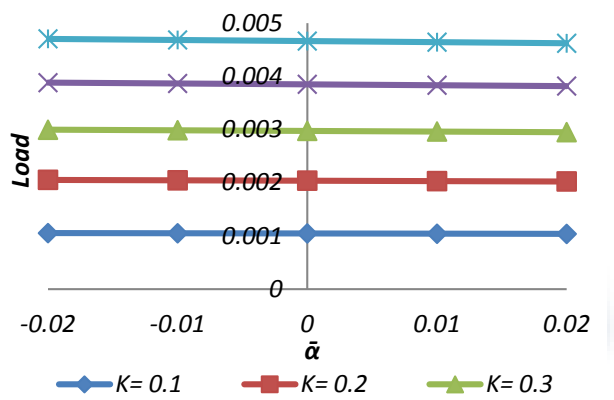
Figure 28: Variation of Load carrying capacity with respect to $\bar{\alpha}$ and K.
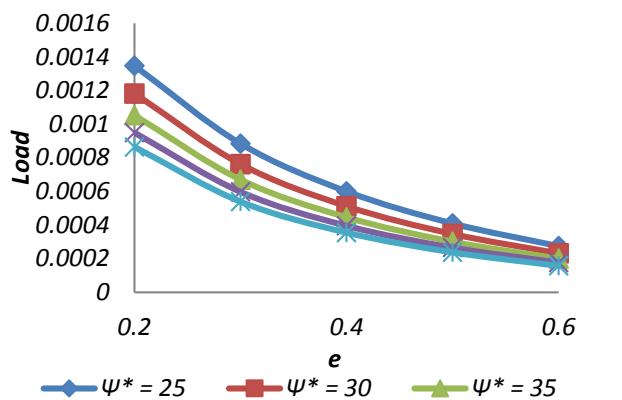
Figure 29: Variation of Load carrying capacity with respect to e and ψ^*.
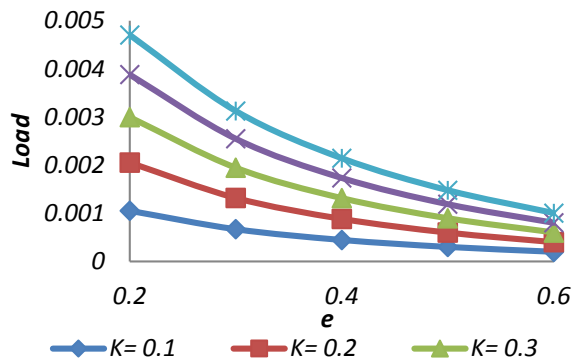
Figure 30: Variation of Load carrying capacity with respect to e and K.
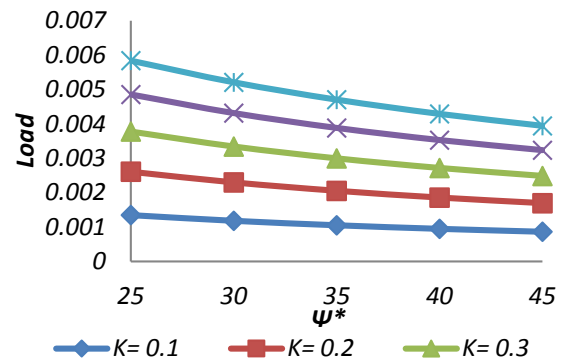
Figure 31: Variation of Load carrying capacity with respect to ψ^* and K.

Figures 2-16 are for the load carrying capacity concerned with Kozeny- Carman's model while the load carrying capacity corresponding to Irmay are presented in Figures 17-31.

The variation of load carrying capacity with respect to standard deviation presented in figures 2-6 and 17-21 makes it clear that the load carrying capacity reduces due to the standard deviation. It is seen that in the case of both the models the effect of skewness on the variation of load carrying capacity with respect to the standard deviation is at the most nominal. Further, the effect of porous structure parameter on the distribution of load carrying capacity with respect to standard deviation is almost negligible in the case of Kozeny-Carman's model. Also, the effect of variance on the variation of load carrying capacity with respect to standard deviation is at the most nominal in the case of Irmay's model.

The effect of skewness is presented in figures 7-10 and 22-25. It is seen that positively skewed roughness decreases the load carrying capacity in the case of both the models but this decrease is more in the case of Kozeny-Carman's model. Besides, the negatively skewed roughness increases the load carrying capacity and this increase is more in Kozeny-Carman's model.

Figures 11-13 and 26-28 depict the distribution of load carrying capacity with respect to the variance. The variance follows almost the path of skewness so far as the trends of load carrying capacity are concerned. However, the effect of porous structure on the variance of load carrying capacity with respect to variance is not that significant in the case of Kozeny-Carman's model. It is interesting to see that at the most the effect of variance is nominal in the case of Irmay's model.

The fact that porosity reduces the load carrying capacity is reflected in figures 14-15 and 29-30. Further, it is seen that the initial combined effect of porosity and porous structure is not that significant in the case of Kozeny-Carman's model.

The nominal increase in the load carrying capacity with respect to porosity is to be found in figures 16 and 31, when considered with film thickness ratio.

In fact a scrutiny of the graphs reveals the following:

1. The load carrying capacity increases owing to the magnetization and this increase is relatively more in the case of Kozeny-Carman's model.
2. The roughness has adverse effect in general but negatively skewed roughness increases the non dimensional load carrying capacity and this gets further increased by the variance(-ve).
3. Porosity affects the bearing system adversely. However, this effect is relatively less in the case of Kozeny-Carman's model.
4. The standard deviation associated with roughness induces a negative effect as load carrying capacity decreases substantially.
5. The negative effect of porosity and standard deviation can be minimized by the positive effect of magnetization in the case of negatively skewed roughness and this reduction is more in the case of Kozeny-Carman's model.
6. The bearing can support a load even when there is no flow, for both the models.

4. CONCLUSIONS

The adverse effect of roughness can be minimized by the positive effect of magnetization and the positive effect of variance negative in the case of Kozeny-Carman's model. The effect of skewness remains superior as compared to the variance for the Kozeny-Carman's model. This article suggests that the roughness aspects must be given due respect while designing the bearing system even if there is the presence of a suitable magnetic strength. The negatively skewed roughness

may go a long way for mitigating the negative effect of porosity in both the models. The Kozeny-Carman's model may be preferred over the Irmay's model for this type of bearing system.

References

[1.]   Adamu, G. and Sinha, P.: Thermal and Roughness Effects in a Tilted Pad Slider Bearing Considering Heat Conduction Through the Pad and Slider, Proceedings of the National Academy of Sciences, India Section A: Physical Sciences, vol. 82(4), pp. 323-333, 2012.

[2.]   Agrawal, V. K.: Magnetic fluid based porous inclined slider bearing, WEAR. 107, 133-139, 1986.

[3.]   Bhat M. V. and Deheri, G. M.: Porous slider bearing with squeeze film formed by a magnetic fluid, Pure and Applied Mathematika Sciences, Vol. 39(1-2), pp. 39-43, 1995.

[4.]   Bhat M. V.: Lubrication with a Magnetic fluid, India, Team Spirit (India) Pvt. Ltd, 2003.

[5.]   Cameron, A.: Basic Lubrication Theory, Ellis Harwood Limited, Halsted Press, John Willy and Sons, New-York, 1972.

[6.]   Capitao, J.W.: Performance characteristics of tilting pad thrust bearings at high operating speeds, Journal of Lubrication Technology, vol. 98(1), pp. 81-88, 1976.

[7.]   Chiang, Hsiu Lu; Chou, Tsu Liang and Yang, Ching Been: Performance Analysis of Magnetic Hydrodynamic Tilted Bearing with Surface Roughness, Advanced Materials Research, vol. 579, pp. 407, 2012.

[8.]   Christensen, H. and Tonder, K. C.: The hydrodynamic lubrication of rough bearing surfaces of finite width, ASME-ASLE Lubrication Conference. Cincinnati. OH. Paper no. 70-lub-7, October 12-15, 1970.

[9.]   Christensen, H. and Tonder, K. C.: Tribology of rough surfaces: stochastic models of hydrodynamic lubrication, SINTEF, Report No.10, pp. 69-18, 1969a.

[10.]   Christensen, H. and Tonder, K. C.: Tribology of rough surfaces: parametric study and comparison of lubrication models, SINTEF, Report No.22, pp. 69-18, 1969b.

[11.]   Deheri, G. M.; Andharia, P. I. and Patel, R. M.: Transversely rough slider bearings with squeeze film formed by a magnetic fluid, Int. J. of Applied Mechanics and Engineering, 10(1), 53-76, 2005.

[12.]   Glavatskih, S.: Steady state performance characteristics of a tilting pad thrust bearing, Journal of Tribology, vol. 123(3), pp. 608-615, 2001.

[13.]   Heinrichson, N.; Fuerst A. and Santos, I. F.: The Influence of Injection Pockets on the Performance of Tilting-Pad Thrust Bearings—Part II: Comparison Between Theory and Experiment, J. Tribol, vol. 129(4), pp. 904-912, 2007.

[14.]   Irmay, S.: Flow of liquid through cracked media, Bull. Res. Counc. Isr, vol. 5A (1), pp. 84, 1955.

[15.]   Liu, J.: Analysis of a porous elastic sheet damper with a magnetic fluid, Journal of Tribolog, vol. 131, pp. 0218011-15, 2009.

[16.]   Majumdar, B.C.: Introduction to Tribology of Bearings, New Delhi, S. Chand & Company Lim., 2008.

[17.]   Patel, J. R. and Deheri, G.: Effect of various porous structures on the Shliomis model based ferrofluid lubrication of the film squeezed between rotating rough curved circular plates, Facta Universitatis, Series: Mechanical Engineering, vol. 12(3), pp. 305-323, 2014.

[18.]   Patel, J. R. and Deheri, G.: Shliomis model based ferrofluid lubrication of squeeze film in rotating rough curved circular disks with assorted porous structures, American journal of Industrial Engineering, vol. 1(3), pp. 51-61, 2013.

[19.]   Patel, J. R. and Deheri, G.: Shliomis model-based magnetic squeeze film in rotating rough curved circular plates: a comparison of two different porous structures, Int. J. Computational Materials Science and Surface Engineering, vol. 6(1), pp. 29–49, 2014.

[20.]   Patel, J. R. and Deheri, G. M.: A comparison of porous structures on the performance of a magnetic fluid based rough short bearing, Tribology in industry, vol. 35(3), pp. 177-189, 2013.

[21.]   Patel, J. R. and Deheri, G. M.: Performance of a magnetic fluid based double layered rough porous slider bearing considering the combined porous structures, Acta Tehnica Corviniensis – Bulletin of Engineering, vol. VII(4), pp. 115-125, 2014.

[22.]   Patel, J. R. and Deheri, G. M.: A Comparison of Different Porous Structures on the Performance of A Magnetic Fluid Based Double Porous Layered Rough Slider Bearing, International Journal of Materials Lifetime, vol. 1(1), pp. 29-39, 2015.

[23.]   Prajapati, B. L.: On Certain Theoretical Studies in Hydrodynamic and Electro-magneto hydrodynamic Lubrication, Ph. D. Thesis: S.P. University, Vallabh Vidya- Nagar, 1995.

[24.]   Shukla, S. D. and Deheri, G. M.: Rough Tilted pad Slider Bearing Lubricated with a Magnetic Fluid, Asian Journal of Science and Technology, vol. 4(11), pp. 034-039, 2012.

[25.]   Sinha, P. and Adamu, G.: THD analysis for slider bearing with roughness: special reference to load generation in parallel sliders, Acta Mechanica, vol. 207(1-2), pp. 11-27, 2009.

[26.]   Wasilczuk, M.: Comparision of an optimum profile hydrodynamic thrust bearing with a typical tilting pad thrust bearing, Lubrication Science, vol. 15(3), pp. 265-273,2003.

[27.]   Yongbin, Z.: A tilted pad thrust slider bearing improved by the boundary slippage, Meccanica, vol. 48(4), pp. 769-781, 2013